ELESTRES: A FINITE ELEMENT FUEL MODEL FOR NORMAL OPERATING CONDITIONS

HENRY H. WONG,* ERTUGRUL ALP,
W. R. CLENDENING,† M. TAYAL,† and LLOYD R. JONES
Westinghouse Canada, Inc., Atomic Power Division, Hamilton Ontario, Canada, L8N 3K2

Received February 1, 1981
Accepted for Publication November 5, 1981

The ELESTRES code is a computer code designed to model the behavior of the Canada deuterium-uranium nuclear fuel elements under normal operating conditions. It models a single element by accounting for the radial and axial variations in stresses and displacements. The constituent models are physically (rather than empirically) based and include such phenomena as fuel-to-sheath heat transfer; temperature and porosity dependence of fuel thermal conductivity; burnup-dependent neutron flux depression; burnup- and microstructure-dependent fission product gas release; and stress-, dose-, and temperature-dependent constitutive equations for the sheath.

The finite element model for the pellet deformation includes thermal, elastic, plastic, and creep strains as well as swelling and densification; pellet cracking; and rapid drop of UO_2 yield strength with temperature. It uses the variable stiffness method for plasticity and creep calculations and combines it with a modified Runga-Kutta integration scheme for rapid convergence and accuracy.

Comparison of code predictions with experimental data indicates good agreement for the calculation of gas release and pellet-midplane and pellet-end sheath strains.

I. INTRODUCTION

The ELESTRES code is designed to model the thermal and mechanical behavior of Canada deuterium-uranium (CANDU) nuclear fuel elements under normal operating conditions. It was developed from the ELESIM fuel performance code[1,2] by replacing the one-dimensional stress-independent fuel expansion model of the latter with a two-dimensional axisymmetric finite element stress analysis of the fuel pellet. The primary motivation for ELESTRES development is to provide more accurate estimates of the effects of stress-dependent processes, in particular, sheath strain during power ramps and the axial variation in strain (due to pellet-end effects). Because the fission product gas release model includes a dependence on pellet stress, some improvement in this calculation was also anticipated.

There are several other fuel performance codes[3-7] developed independently that share some common features with ELESTRES. The purpose of the present paper is not to make a detailed comparison of the features of these codes, but to report a portion of the Canadian fuel modeling efforts in recent years.

In the two previous papers on ELESIM by Notley,[1,2] the models for such phenomena as fuel-to-sheath heat transfer, temperature and porosity dependence of fuel thermal conductivity, burnup-dependent neutron flux depression, burnup- and microstructure-dependent fission gas release, fuel thermal expansion, swelling, and densification have all been described. In the present paper, attention is focused on the ELESTRES equations governing the thermal and mechanical behavior of the fuel element, the approximations, boundary conditions, and methods of solution. Individual models for the above phenomena are referenced at appropriate times.

*Present address: Ontario Hydro, 700 University Avenue, Toronto, Ontario M5G 1X6, Canada.
†Present address: Atomic Energy of Canada Limited, Sheridan Park Research Community, Mississauga, Ontario, L5K1B2, Canada.

Comparison of the code's predictions of sheath strains and gas release with ELESIM predictions and experimental data is presented.

I.A. Problem Description

Our main objective is to develop a model that can be utilized to predict effects of changes in design parameters on nuclear fuel performance. The two major variables of interest are the sheath strain and gas release in a single fuel element. The element is subjected to reactor coolant conditions and a neutron flux that, in general, has a nonuniform distribution in the axial direction as well as in the radial direction across the fuel element. To reduce the size of the modeling problem, several basic simplifications have been made; it is assumed that there is no axial neutron flux variation and that axisymmetry exists within the element. These simplifications allow us to use two- or even one-dimensional models instead of three-dimensional ones.

Let us now consider the geometry as shown in Fig. 1. The UO_2 pellets, in the form of right circular cylinders, are clad in a thin-walled Zircaloy-4 sheath. The bombardment of UO_2 by neutrons results in the release of thermal energy. This energy is conducted out of the UO_2 fuel, across the fuel-sheath gap, the sheath, and transferred to the coolant (Fig. 2). The coolant is under high pressure. To compute the deformations in the fuel element, we must solve the static equilibrium equations (mechanical problem) in the pellet and the sheath. The pellets deform under the influences of thermal expansion, densification, swelling, and external forces, and interact with adjacent pellets and the sheath. A major driving force in pellet deformation is that due to temperature gradients. Hence, we must solve for the temperature distribution in the fuel element (thermal problem) before we can proceed with the mechanical problem. These two problems are fundamental in the analysis of fuel behavior. We shall now examine the method of solution of each problem together with how they interact and affect each other.

II. GOVERNING EQUATION AND SOLUTION METHOD FOR THE THERMAL PROBLEM

The temperature field within the pellet and the sheath is approximated as one dimensional, since axisymmetry and no axial neutron flux variation in an element are assumed. This analysis is identical to the one used in ELESIM. The governing differential equation for conduction heat flow in a solid circular cylinder (UO_2 pellet) with internal heat generation can be written as

$$\frac{d}{dr}\left(k\frac{dT}{dr}\right)+h=0\ , \tag{1}$$

where

k = thermal conductivity

r = radial coordinate

T = temperature

h = heat generation rate per unit volume.

The boundary conditions are

$$\left.\frac{dT}{dr}\right|_{r=0}=0 \tag{2}$$

and

$$T(r=a)=T_{p0}\ ,$$

where a is the outer radius of the pellet and T_{p0} is the temperature at the pellet surface. At any point in time $t = t_0$, the coolant temperature and element

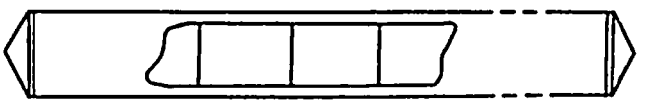

Fig. 1. Geometry of fuel element to be modeled.

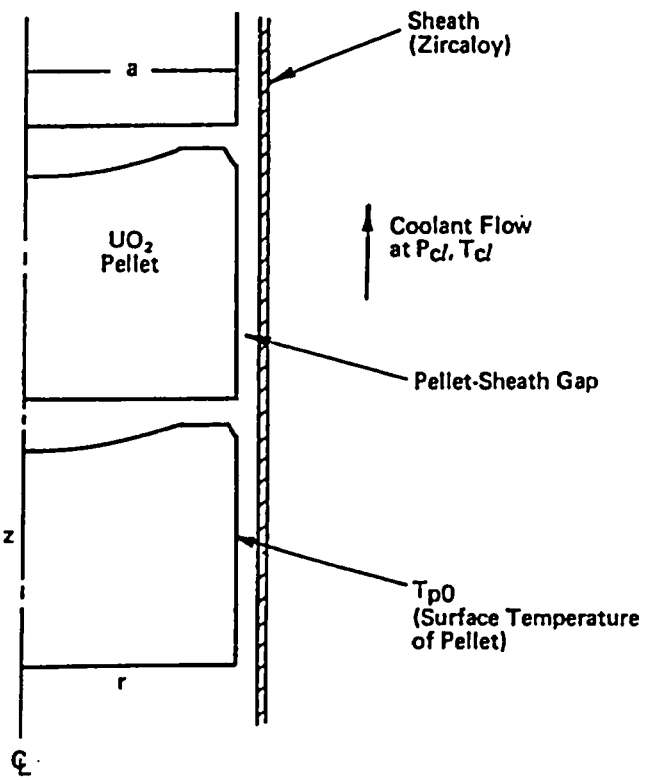

Fig. 2. Radial-axial cross section of the fuel element.

power are assumed known. If the sheath-coolant film coefficient and the pellet-sheath heat transfer coefficient are known, T_{p0} can be accurately estimated by performing simple heat balances. In ELESTRES, thermal conductivities of UO_2 and Zircaloy are modeled using equations recommended in MATPRO (Ref. 8). The internal heat generation rate is modeled using an equation for the neutron flux distribution that was recommended by Robertson[9] and later modified to account for the neutron flux depression across the fuel radius.[2] The film coefficient may be input at various times along the power history. The fuel-sheath total heat transfer coefficient is computed using equations originally suggested by Ross and Stoute[10] and modified by Campbell et al.[11]

Because of the nonlinearities involved in the coefficients, Eq. (1) is solved numerically using a simple finite difference scheme.

III. GOVERNING EQUATIONS AND SOLUTION METHOD FOR THE MECHANICAL PROBLEM

III.A. Governing Equations of Static Equilibrium for the Pellet

The stress and displacement fields within the pellet are approximated in this analysis as being symmetric about the central axis and about the midplane. Azimuthal independence reduces the dimensionality of the problem from three to two, namely, from (r,θ,z) to (r,z) and leads to $\partial/\partial\theta = v = 0$, where $\partial/\partial\theta$ is the variation with respect to θ, and v is the displacement in the θ direction. The resulting governing equations of static equilibrium for the pellet are solved using the finite element method. A mesh of 54-56 triangular finite elements (Fig. 3) is used to represent a quarter pellet with or without a dish, land, and chamfer.

The elemental finite element equation based on a force balance is derived following the displacement approach given in Zienkiewicz[12]:

$$\{F\}^e = [K]^e\{\delta\}^e + \{F\}^e_{\epsilon_0} + \{F\}^e_{\sigma_0} \quad . \tag{3}$$

Here,

$$[K]^e = \iiint_V [B]^T[D][B]dV \quad , \tag{4}$$

$$\{F\}^e_{\epsilon_0} = -\iiint_V [B]^T[D]\{\epsilon_0\}dV \quad , \tag{5}$$

and

$$\{F\}^e_{\sigma_0} = \iiint_V [B]^T\{\sigma_0\}\,dV \quad , \tag{6}$$

where

$\{F\}^e$ = nodal forces that are statically equivalent to the boundary stresses and distributed loads on the element

$[K]^e$ = elemental stiffness matrix that relates nodal displacements $\{\delta\}^e$ to nodal forces

$\{F\}^e_{\epsilon_0}$ = nodal forces due to initial strains $\{\epsilon_0\}$

$\{F\}^e_{\sigma_0}$ = nodal forces due to initial stresses $\{\sigma_0\}$

$[B]$ = matrix relating displacements to strains in an element,

$$\{\epsilon\}^e = [B]\{\delta\}^e \tag{7}$$

$[D]$ = matrix relating strains to stresses in an element,

$$\{\sigma\}^e = [D]\{\epsilon\}^e \quad . \tag{8}$$

The global set of finite element equations is assembled from the elemental finite element equations following a standard procedure. The global equations have the same form as Eq. (3), i.e.,

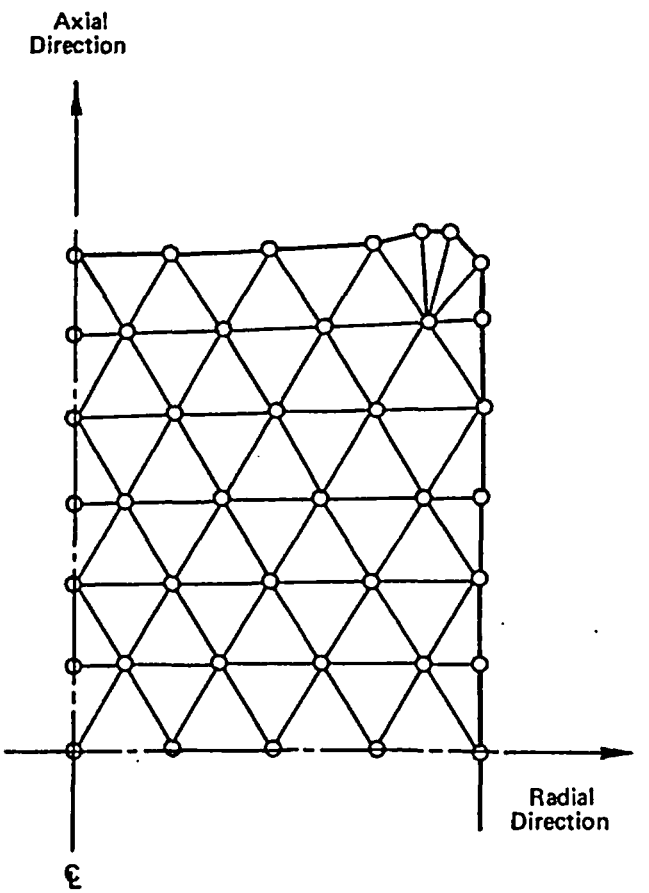

Fig. 3. Two-dimensional axisymmetric finite element representation of a segment of a radial-axial cross section of a fuel pellet.

$$\{F\} = [K]\{\delta\} + \{F\}_{\epsilon_0} + \{F\}_{\sigma_0} , \quad (9)$$

except that the superscript e has been dropped to denote that this equation is valid for the whole body. After the assembly is carried out, each member of $\{F\}$ is equal to the sum of the component forces contributed by the elements meeting at that node. This in turn must equal the external concentrated forces (which may be zero) at the nodes in order to satisfy the static equilibrium requirement. Hence, if we denote the set of external concentrated forces at the nodes as $\{R\}$, Eq. (9) becomes

$$\{R\} = [K]\{\delta\} + \{F\}_{\epsilon_0} + \{F\}_{\sigma_0} . \quad (10)$$

This equation can be solved to give the nodal displacements. Using Eqs. (7) and (8), the strains and stresses in each element can then be calculated.

The above equations are equally valid for linear and nonlinear problems. In ELESTRES, the presence of plasticity and creep behavior renders the problem nonlinear. Thus, the quantities $\{R\}$, $\{\delta\}$, $\{F\}_{\epsilon_0}$, and $\{F\}_{\sigma_0}$ are taken as incremental external forces, nodal displacements, and nodal forces due to initial incremental strains and stresses, respectively. The total values of nodal displacements and strains and stresses are simply the sum of the current increment and the previous total.

To solve Eq. (10), we must specify the appropriate displacement and force boundary conditions, nodal forces due to initial strains and stresses, and constitutive equations.

III.B. Nodal Displacement and Force Boundary Conditions for the Pellet

The nodes in the mesh can be classified as either interior or boundary nodes. The boundary nodes have prescribed displacements or external forces.

The nodes along the centerline are constrained to have zero incremental radial displacement. Due to geometric symmetry, they also have zero incremental external axial force.

The nodes along the midplane have zero incremental axial displacement initially and zero external radial force. If, at any time during the calculations, a tensile axial force develops at a midplane node, an axial crack is allowed to develop. A crack may "heal" if the cracked node returns to its original position at a later time.

The nodes facing the sheath have incremental loads due to the pellet-sheath interfacial pressure, which is calculated by performing a force balance on the sheath (Section III.G).

The nodes facing the adjacent pellet are constrained according to the type of interaction among the two pellets and the sheath: (a) no pellet-pellet interaction, (b) pellet-pellet interaction resulting in relative axial slip between the pellets and the sheath, (c) pellet-sheath axial interaction with no relative slip and no axial sheath yielding, and (d) pellet-sheath axial interaction with no relative slip and with axial sheath yielding. The appropriate type of interaction is determined by the amount of axial clearance between two adjacent pellets, total axial gap in the element, and the axial force required to yield the sheath.

III.C. Nodal Incremental Forces Due to "Initial" Strains in the Pellet

The incremental strains due to temperature changes and irradiation induced densification and swelling for the current time step are considered as incremental "initial" strains. The thermal strain increment is calculated using the same model for the thermal expansion coefficient as in ELESIM, and densification and swelling strains are modeled as described by Notley.[2] The respective nodal forces are then calculated using Eq. (5) and utilized in Eq. (3).

III.D. Nodal Incremental Forces Due to "Initial" Stresses in the Pellet

Incremental stresses arising due to pellet radial cracking (tensile hoop stress), temperature associated changes in flow stress, and material creep are considered as incremental "initial" stresses.

III.D.1. Initial Stresses Arising from the Pellet Radial Cracking Model

The ELESTRES code simulates radial cracking by enforcing a "plane" stress deformation mode on those finite elements that have been identified as cracked. The [D] matrix in the σ-ϵ constitutive equation [Eq. (8)] is modified to give zero hoop stress for a cracked element. Only elements whose centroidal radii are greater than a limiting radius and whose hoop stresses exceed the fracture stress are allowed to crack radially. Besides the change in the element stiffness matrix $[K]^e$ when an element cracks radially, the hoop stress that is present in the element prior to the formation of the radial crack must be accounted for. The correction takes the form of an "initial" stress. The procedure in ELESTRES parallels that given by Zienkiewicz.[13] The incremental forces resulting from these initial stresses are equal to [from Eq. (6)]

$$\{F\}^e_{\sigma_0} = \iiint_V [B]^T \begin{Bmatrix} 0 \\ -\sigma_\theta \\ 0 \\ 0 \end{Bmatrix} dV . \quad (11)$$

These nodal forces are then utilized in Eq. (3).

III.D.2. Initial Stresses Arising from a Reduction in Flow Stress

Incremental initial stresses may also arise from a reduction in the flow stress associated with a temperature increase in an element. The appropriate stress correction $\{\sigma_0\}$ is

1. for a radially uncracked element:

$$\{\sigma_0\} = \frac{d\tilde{\sigma}}{\bar{\sigma}} \{\sigma'\} , \quad (12)$$

where

$\bar{\sigma}$ = effective stress

$d\tilde{\sigma}$ = difference between the effective stress $\bar{\sigma}$ and the uniaxial yield stress $\tilde{\sigma}$

σ' = deviatoric stresses;

2. for a radially cracked element:

$$\{\sigma_0\} = \frac{2}{3} \bar{\sigma} d\tilde{\sigma} \{S'\} , \quad (13)$$

where

$$\{S'\} = \left\{\frac{S_1}{S}, 0, \frac{S_3}{S}, \frac{S_4}{S}\right\} T$$

$$S = \sigma'_r S_1 + \sigma'_z S_3 + 2\tau_{rz} S_4$$

$$S_1 = \frac{E}{1-\nu^2} (\sigma'_r + \nu\sigma'_z)$$

$$S_3 = \frac{E}{1-\nu^2} (\nu\sigma'_r + \sigma'_z)$$

$$S_4 = \frac{E}{1+\nu} \tau_{rz} . \quad (14)$$

The terms E and ν are the Young's modulus and Poisson's ratio, respectively.

III.D.3. Initial Stresses Arising from the Creep Model

Material creep gives rise to an incremental initial stress term with magnitude

$$\{\sigma_0\} = \frac{3}{2} C dt [\mathbf{D}][\mathbf{j}]\{\sigma'\} , \quad (15)$$

where

C = creep function $\dot{\epsilon}/\bar{\sigma}$

$\dot{\epsilon}$ = creep strain rate, defined by an equation suggested by Armstrong[14]

$\bar{\sigma}$ = effective stress

dt = time increment

$$[\mathbf{j}] = \begin{bmatrix} 1 & 0 & 0 & 0 \\ 0 & 1 & 0 & 0 \\ 0 & 0 & 1 & 0 \\ 0 & 0 & 0 & 2 \end{bmatrix} \quad (16)$$

$[\mathbf{D}]$ = elasticity matrices for elements exhibiting creep behavior.

The elasticity matrices for elements exhibiting creep behavior are presented later. To take large time intervals in a single calculation of incremental displacements due to creep, the incremental initial stress term is modified for those finite elements that exhibit a very rapid relaxation of their stresses. These elements are treated as if they exhibit a pure stress relaxation of their effective stresses (constant total strain). The resulting incremental initial stresses for these elements are

$$\{\sigma_0\} = \frac{3}{2} \frac{1}{E} \{1 - \exp[-CE(dt)]\} [\mathbf{D}][\mathbf{j}]\{\sigma'\} , \quad (17)$$

where the quantities are defined as in Eq. (15) except that $[\mathbf{D}]$ is the elasticity matrix for elements exhibiting elastic behavior.

III.E. Pellet Constitutive Equations Relating Incremental Strains to Incremental Stresses

The only term that remains to be defined in Eq. (10) is the global stiffness matrix $[\mathbf{K}]$. From Eq. (4), it can be seen that the elemental stiffness matrix $[\mathbf{K}]^e$ depends on $[\mathbf{B}]$ and $[\mathbf{D}]$. Matrix $[\mathbf{B}]$, the coefficient matrix relating displacements to strains, can be easily derived for given shape functions. Matrix $[\mathbf{D}]$, the coefficient matrix relating strains to stresses, will vary depending on the type of behavior exhibited by the finite element (e.g., elastic, elastic-plastic, or time-dependent creep). Matrix $[\mathbf{D}]$ has to be derived for each case using the following constitutive equations: (a) Hooke's Law, (b) Hencky-Von Mises yield function, and (c) Prandtl Reuss' plastic flow rule.

Table I summarizes the different $[\mathbf{D}]$ matrices corresponding to the various material behavior that an element may exhibit.

The static equilibrium equations for the pellet are now ready to be solved. In the preceding four sections, the finite element equations for the pellet, the incremental nodal force and displacement constraints, and the constitutive equations have been presented. In the next section, the solution procedure is discussed.

III.F. Solution Procedure for the Pellet

The basic approximation in this solution procedure is that the pellet behavior, influenced by continuous temperature changes during a time interval corresponding to a given burnup increment and linear power, can be simulated sequentially as two independent types of behavior; namely, instantaneous deformation due to instantaneous changes in temperature, and isothermal, time-dependent deformation due to fuel swelling, densification, and creep. In ELESTRES, up to eight sequential

TABLE I

Summary of the Different [D] Matrices Corresponding to the Various Material Behavior That an Element May Exhibit

[D]	Uncracked Radially	Cracked Radially
Elastic behavior	$[D]^e = \frac{E}{(1+\nu)(1-2\nu)} \begin{bmatrix} 1-\nu & \nu & \nu & 0 \\ \nu & 1-\nu & \nu & 0 \\ \nu & \nu & 1-\nu & \\ 0 & 0 & 0 & \frac{1-2\nu}{2} \end{bmatrix}$	$[D]^{e,ck} = \frac{E}{1-\nu^2} \begin{bmatrix} 1 & 0 & \nu & 0 \\ 0 & 0 & 0 & 0 \\ \nu & 0 & 1 & 0 \\ 0 & 0 & 0 & \frac{1-\nu}{2} \end{bmatrix}$
Instantaneous plastic flow behavior	$[D]^p = [D]^e - \frac{3}{2\bar{\sigma}}\left(\frac{E}{1+\nu}\right)\{\sigma'\}\{\sigma'\}^T$, where $\bar{\sigma}$ = effective stress, σ' = deviatoric stresses	$[D]^{p,ck} = [D]^{e,ck} - S\{S'\}\{S'\}^T$, where $S = \sigma_r' S_1 + \sigma_z' S_3 + 2\tau_{rz} S_4$, $\{S'\}^T = \left\{\frac{S_1}{S}, 0, \frac{S_3}{S}, \frac{S_4}{S}\right\}$, $S_1 = \frac{E}{1-\nu^2}(\sigma_r' + \nu\sigma_z')$, $S_3 = \frac{E}{1-\nu^2}(\nu\sigma_r' + \sigma_z')$, $S_4 = \frac{E}{1+\nu}\tau_{rz}$
Time-dependent creep behavior	$[D]^{creep} = \frac{1}{d} \begin{bmatrix} a^2-b^2 & b(b-a) & b(b-a) & 0 \\ b(b-a) & a^2-b^2 & b(b-a) & 0 \\ b(b-a) & b(b-a) & a^2-b^2 & 0 \\ 0 & 0 & 0 & \frac{d}{c} \end{bmatrix}$, where $a = \frac{1}{E} + \frac{C}{2}dt$, $b = \frac{\nu}{E} - \frac{C}{4}dt$, $c = \frac{2(1+\nu)}{E} + 1.5Cdt$, $d = a(a^2-b^2) + 2b^2(b-a)$, dt = time increment (h) , C = creep function $(\dot{\epsilon}/\bar{\sigma})$, $\bar{\sigma}$ = effective stress (Pa) .	$[D]^{creep,ck} = \frac{1}{(b^2-a^2)} \begin{bmatrix} -a & 0 & b & 0 \\ 0 & 0 & 0 & 0 \\ b & 0 & -a & 0 \\ 0 & 0 & 0 & \frac{b^2-a^2}{c} \end{bmatrix}$,
Elastic and plastic behavior	$[D]^{ep} = R'[D]^e + (1-R')[D]^p$, where R' is an estimate of the fraction of stress increment during which the element behaves elastically.	$[D]^{ep,ck} = R'[D]^{e,ck} + (1-R')[D]^{p,ck}$, where R' is an estimate of the fraction of stress increment during which the element behaves elastically.

calculations of incremental displacement are performed to simulate the pellet behavior during a time interval corresponding to a given burnup and linear power. The first three sequential calculations are designed to give pellet deformation due to instantaneous temperature changes and the remaining five calculations are designed to give pellet deformation due to time-dependent creep. Therefore, in each of these eight sequential calculations, only some of the incremental forces due to incremental initial strains and stresses are applied. The global set of equations [Eq. (10)] is solved by Gaussian elimination. The calculations are repeated if the results violate the assumed states of pellet-pellet interaction and pellet axial cracking. Otherwise the resulting incremental displacement and stress fields are added to the previous totals to give current total displacement and stress fields.

III.G. Governing Equation of Static Equilibrium for the Sheath

Consider now the static equilibrium problem for the sheath. The analysis is carried out by performing independent one-dimensional force balances at seven axial locations along the pellet length. The pellet is assumed to be rigid (temporarily) and any interaction between the sheath and the pellet is taken care of through the use of interfacial pressure. The force balance on the sheath is written as:

$$2t_s\sigma_h = (P_g + P_i - P_{cl})D \ , \qquad (18)$$

where

t_s = sheath thickness

σ_h = sheath hoop stress

P_g = internal gas pressure

P_i = pellet-sheath interfacial pressure

P_{cl} = coolant pressure

D = current internal sheath diameter.

Here, the stresses in the axial and radial directions are not considered. The constitutive equation which relates the stresses to the strains is given by Hosbons et al.,[15] Coleman et al.,[16] and Holt et al.[17] In this model the expressions for strain rate include strain rate sensitivity, work hardening, irradiation hardening, and strain softening. The elastic and plastic (including primary and secondary creep) strain components are calculated for given hoop stress, time increment, sheath temperature, neutron dose, and flux conditions.

The sheath thickness and the coolant pressure are both input parameters. The internal gas pressure is calculated from the initial filling gas volume at STP, the volume of fission gas released at STP, and the voidage available for gas storage. The fission gas release is calculated using the model described by Notley and Hastings.[18] The interfacial pressure and hoop stress calculations depend on the existence of a pellet-sheath gap. If the gap exists, then the interfacial pressure is zero and the sheath strains can be calculated from known hoop stress [Eq. (18)]. If the gap does not exist, then the internal diameter of the sheath is set equal to the current pellet diameter. The interfacial pressure is then obtained from Eq. (18), using a secant iteration scheme.

We have now covered the solution methods to the thermal and mechanical problems at any given time $t = t_0$. To simulate fuel behavior under an arbitrary power history, the calculations are sequenced using a history model. This model is discussed next.

IV. THE HISTORY MODEL

Consider the idealized power history as shown in Fig. 4. The linear power, ramp rate or ramp time, and burnup or time at power are the quantities that must be supplied at predetermined points along the power history. Central to this model is the idea that the fuel is subjected to either instantaneous power changes or constant power operation. The ramp rate (or time) supplied during input is used only in determining an appropriate time interval, after an instantaneous power change, during which stress relaxation and creep are allowed to take place. It can be seen (from Fig. 4) that if the power change between one history point and the next is taken as a series of smaller power changes, the power history can be more accurately followed. The stress field will also be more accurate since the smaller steps can prevent the excessive buildup of stresses before stress relaxation is allowed to occur. Therefore, to maintain computation accuracy, there is a maximum allowable power change in any one single calculation of fuel behavior. During constant power operation, the fuel behavior is expected to change at a much slower rate than during a power change, hence much longer burnup increments may be taken. In ELESTRES, if the burnup increment supplied exceeds a predetermined maximum, the calculations related to stress relaxation and creep are performed

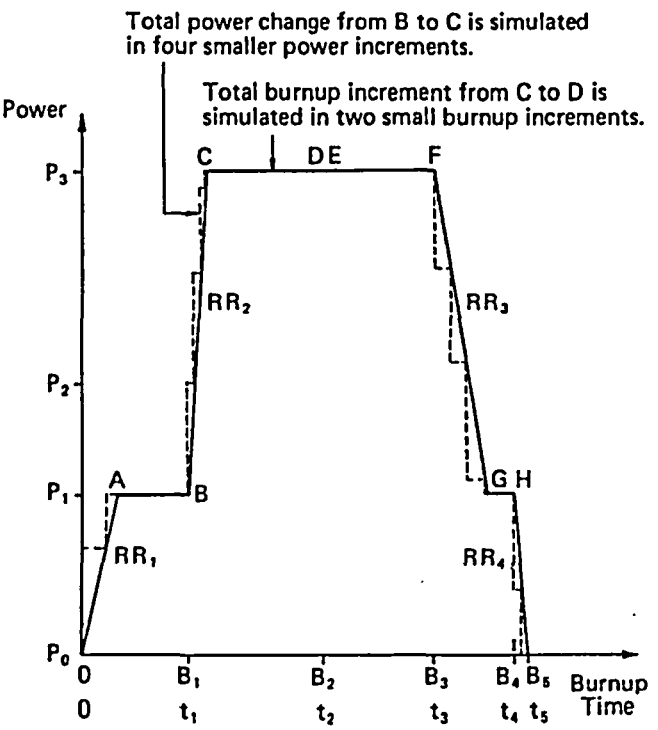

Fig. 4. Sample power history.

once at the very end of the total burnup increment, but the thermal solution and the gas release calculations are performed repeatedly at every maximum allowable increment. The strategy employed here ensures computational efficiency as well as accuracy in gas release predictions.

The calculation sequence in ELESTRES can be broadly divided up into three parts: inputs and initialization, calculation of fuel behavior, and outputs. In inputs and initialization, the as-fabricated fuel geometry, material properties, and the initial operating conditions are defined. In the calculation of fuel behavior, the fuel defect probabilities, ramp rate, and power increment are defined for those calculations of fuel behavior subjected to power changes. For calculations of fuel behavior subjected to constant power operation, the appropriate burnup increment is defined. The solution to the thermal problem follows. This includes the calculations of heat generation rate, sheath temperatures, sheath and fuel material properties, and the temperature distribution within the UO_2 pellet. Using the current temperature distribution, the amount of fission gas arriving at the grain boundaries via molecular diffusion and grain boundary sweeping is calculated. This last calculation is not performed for burnup increments associated with power changes because the time available for these processes to occur is short and the amount of gas arriving at the grain boundaries is considered negligible.

The volume of gas released into the voidage is calculated as the difference between the total amount of gas that has arrived at the grain boundaries since the start of the history and the amount of gas that can be retained, in the form of gas bubbles, at the grain boundaries under present reactor and fuel conditions. The solution to the mechanical problem begins with the calculation of densification and swelling strains. The finite element analysis of stress-strain is performed for all burnups associated with power changes, but it is performed only once at the end of the supplied burnup increment associated with constant power operation. Using the new pellet geometry, the sheath stresses and strains are calculated. A new total fuel to sheath heat transfer coefficient is next defined before control is returned to the beginning of the next calculation of fuel behavior. The gas pressure, sheath strains, center temperature, percentage gas release, etc. are output at the end of supplied power changes and burnup increments (i.e., at points A, B, C, . . . , I on Fig. 4). Calculations proceed until the end of the supplied power history is reached.

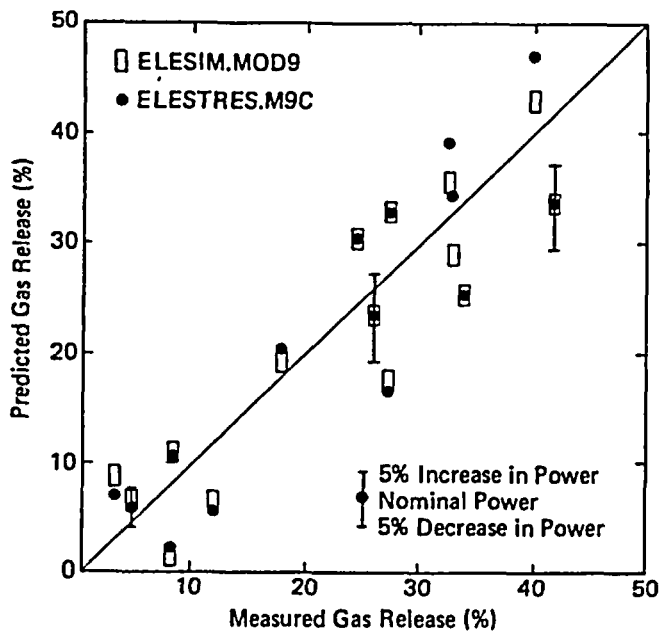

Fig. 5. Gas release comparisons.

V. COMPARISON OF ELESTRES PREDICTIONS WITH EXPERIMENTAL DATA AND WITH ELESIM PREDICTIONS

The ELESTRES code was run for 18 cases covering a wide range of power-burnup histories. Predictions of percent gas release, diametral sheath strain at pellet midplane and at pellet end, all taken at the end of power history, are compared with the ELESIM predictions and available experimental data.

Figure 5 shows a comparison of predicted versus measured percent gas release. It can be seen that the predictions of ELESTRES and ELESIM are very similar. It should be noted that the small amount of "fine tuning" of the gas diffusion coefficient performed in ELESIM (Ref. 2) was not required in ELESTRES to obtain comparable percent gas release predictions. This is mainly due to differences in the calculation of stresses used in the gas release model. In general, the calculated values, making allowance for a ±5% power uncertainty, compare well to experimental values.

Figure 6 shows the final plastic sheath strain comparisons for the pellet midplane and pellet end. The ELESTRES sheath strain prediction variations due to a ±5% change in power are also shown. In general, the agreement is quite reasonable between predicted and measured plastic sheath strains when the limits of power estimate and measurement accuracy are both considered.

Table II summarizes some simple statistics with regard to the above comparisons. It can be seen that ELESTRES predicts gas release as well as ELESIM without the "fine tuning" mentioned above, and in addition it has the capability of computing the circumferential ridges. This is accomplished with a

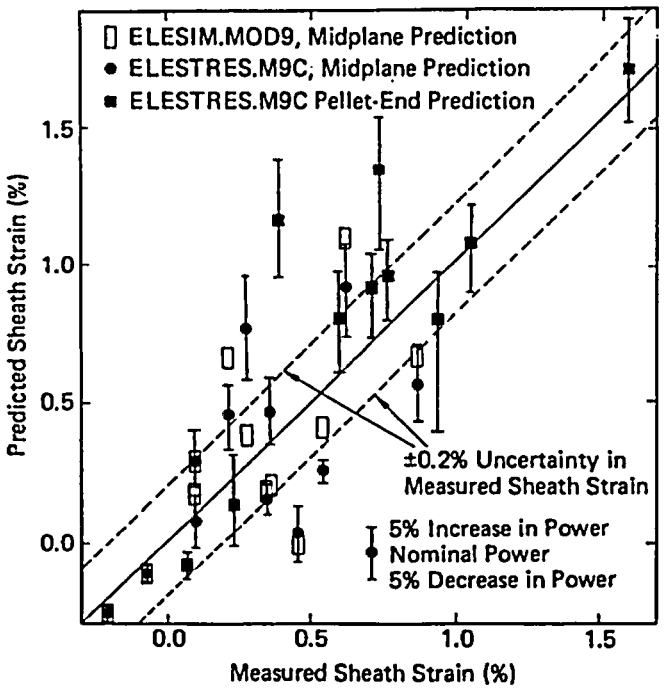

Fig. 6. Comparison of predicted versus measured final plastic sheath strains.

relatively small penalty (a factor of 3 to 7) in terms of the computation time.

VI. SUMMARY AND CONCLUSIONS

The ELESTRES fuel performance code simulates fuel element behavior under normal operating conditions with one- and two-dimensional physically based models. The principles of conservation of energy and conservation of momentum are applied in the form of the heat conduction and the static equilibrium equations for the analysis of fuel behavior. To solve for the fuel temperature, a one-dimensional finite difference method is used. A two-dimensional finite element method is employed for the pellet stresses and strain in conjunction with one-dimensional calculations for deformations in the sheath.

The ELESTRES predictions of percent gas release and final sheath strains are compared with ELESIM predictions and with experimental data. The predictions are found to be in good agreement with the experimental data.

ACKNOWLEDGMENTS

The efforts of M. J. F. Notley of Atomic Energy of Canada Limited (AECL) in the initiation and development of this program are gratefully acknowledged. We also appreciate the encouragement by Ontario Hydro and AECL personnel for the publication of this work.

The work presented here is part of a continuing program at Westinghouse Canada, Inc., Atomic Power Division, and was funded by AECL and Ontario Hydro.

TABLE II

Statistics of the (Predicted-Experimental) Deviations of Results Based on Nominal Power

Predicted-Experimental	ELESIM	ELESTRES
Gas release (%)		
Mean[a]	−1.5	−1.3
2σ[b]	10.9	12.0
Final sheath strain at pellet midplane (%)		
Mean[a]	0.0	0.0
2σ[b]	0.5	0.5
Final sheath strain at pellet end (%)		
Mean[a]	N/A	0.2
2σ[b]	N/A	0.6

[a]Mean = mean deviation

$$= \sum_{i}^{N} (\text{predicted-experimental})_i / N.$$

[b]σ = standard deviation

$$= \left\{ \sum_{i}^{N} [(\text{predicted-experimental})_i - \text{mean}]^2 / N \right\}^{1/2}.$$

REFERENCES

1. M. J. F. NOTLEY, "A Computer Program to Predict the Performance of UO_2 Fuel Elements Irradiated at High Power Outputs to a Burnup of 10,000 MWd/MTU," *Nucl. Appl. and Technol.*, **9**, 195 (1970).

2. M. J. F. NOTLEY, "ELESIM: A Computer Code for Predicting the Performance of Nuclear Fuel Elements," *Nucl. Technol.*, **44**, 445 (1979).

3. M. KINOSHITA and M. ICHIKAWA, "Fuel Rod Deformation Code FEMAXI-II and Its Application," *Nucl. Eng. Des.*, **56**, 49 (1980).

4. Y. IWANO, "MIPAC, A Computer Code for Fuel Performance Analysis by the Finite Element Method," *Nucl. Eng. Des.*, **56**, 41 (1980).

5. K. ITO, M. ISHIDA, and M. OGUMA, "'FEAST,' A Finite Element Computer Code for Analysis of the Thermo-Mechanical Fuel Rod Behaviour," Enlarged Halden Programme Group Meeting, Loen, Norway (1978).

6. M. ICHIKAWA, T. OKUBO, Y. IWANO, K. ITO, K. KASHIMA, H. SAITO, and T. NAKAJIMA, "FEMAXI-III: An Axisymmetric Finite Element Computer Code for the Analysis of Fuel Rod Performance," *IAEA Specialists' Mtg. Water Reactor Fuel Element Performance Computer Modeling*, Blackpool, U.K. (1980).

7. K. ITO, Y. WAKASHIMA, and M. OGUMA, "Pellet Compliance Model Based on Out-of-Pile Simulation," *Nucl. Eng. Des.*, **56**, 117 (1980).

8. P. E. MacDONALD and L. B. THOMPSON, "MATPRO-Version 09, A Handbook of Material Properties for Use in the Analysis of Light Water Reactor Fuel Rod Behaviour," Idaho National Engineering Laboratory (1976).

9. J. A. L. ROBERTSON, "$\int kd\theta$ in Fuel Irradiations," AECL-807, Atomic Energy of Canada Limited (1959).

10. A. M. ROSS and R. L. STOUTE, "Heat Transfer Coefficient Between UO_2 and Zircaloy-2," AECL-1552, Atomic Energy of Canada Limited (1962).

11. F. B. CAMPBELL, L. R. BOURQUE, R. DESHAIES, H. E. SILLS, and M. J. F. NOTLEY, "In-Reactor Measurement of Fuel-to-Sheath Heat Transfer Coefficients Between UO_2 and Stainless Steel," AECL-5400, Atomic Energy of Canada Limited (1977).

12. O. C. ZIENKIEWICZ, *The Finite Element Method in Engineering Science*, McGraw-Hill Book Company, New York (1971).

13. O. C. ZIENKIEWICZ, "Stress Analysis of Rock as a 'No Tension' Material," *Geotechnique*, **18**, 56 (1968).

14. W. ARMSTRONG, "Creep Deformation of Stoichiometric Uranium Oxide," *J. Nucl. Mater.*, **7**, 133 (1962).

15. R. R. HOSBONS, C. E. COLEMAN, and R. A. HOLT, "Numerical Simulation of Tensile Behaviour of Nuclear Fuel Cladding Materials," AECL-5245, Atomic Energy of Canada Limited (1975).

16. C. E. COLEMAN, R. A. HOLT, and R. R. HOSBONS, "Numerical Calculation of Plastic Instability During Tensile Deformation," AECL-5429, Atomic Energy of Canada Limited (1976).

17. R. A. HOLT, R. R. HOSBONS, and C. E. COLEMAN, "Simulation of Nuclear Fuel Sheath Deformation Following Fuel Power Transients," AECL-5430, Atomic Energy of Canada Limited (1976).

18. M. J. F. NOTLEY and I. J. HASTINGS, "A Microstructure-Dependent Model for Fission Product Gas Release and Swelling in UO_2 Fuel," AECL-5838, Atomic Energy of Canada Limited (1978).